

Top Dielectric Induced Ambipolarity in an n-channel dual-gated Organic Field Effect Transistor

Kaushik Bairagi^{a,*}, *Elisabetta Zuccatti*^a, *Francesco Calavalle*^a, *Sara Catalano*^a,
Subir Parui^{a,†}, *Roger Llopis*^a, *Frank Ortmann*^b, *Fèlix Casanova*^{a,c}, *Luis E. Hueso*^{a,c,*}

^a CIC nanoGUNE, 20018 San Sebastian, Spain

^b Center for Advancing Electronics Dresden and Dresden Center for Computational Materials Science, Technische Universität Dresden, 01062, Dresden, Germany

^c IKERBASQUE, Basque Foundation for Science, 48013 Bilbao, Spain

† Present address: IMEC and K. U. Leuven, Leuven 3001, Belgium

*E-mail: k.bairagi@nanogune.eu; l.hueso@nanogune.eu

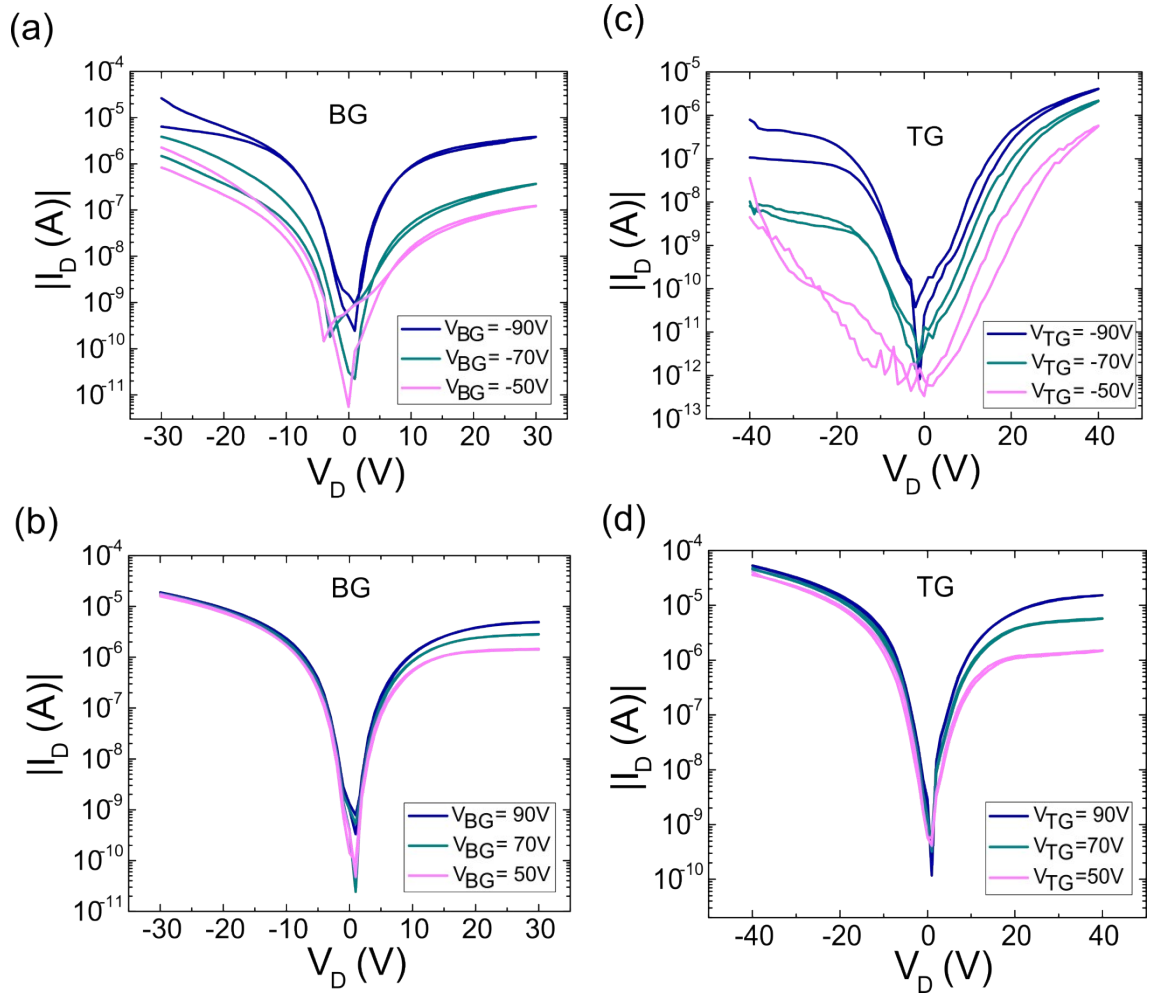


Figure S1. Trace-retrace drain characteristics ($I_D - V_D$) of N2200 (36 nm) transistor when probed with respect to bottom gate (a) for p-type operation (b) for n-type operation and when probed with respect to top gate (c) for p-type operation (d) for n-type operation.

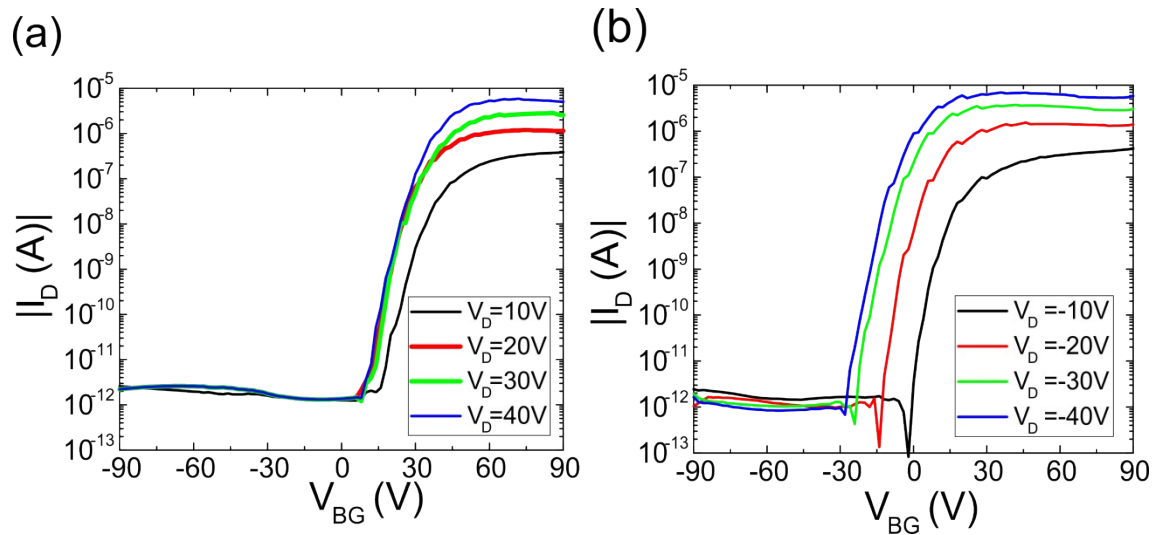


Figure S2. Transfer characteristics of N2200 (115 nm) (baked at 130°C for 1h 30 min) transistor ($L=10 \mu\text{m}$, $W = 10 \text{ nm}$) probed with respect to bottom gate (a) positive V_D (b) negative V_D .

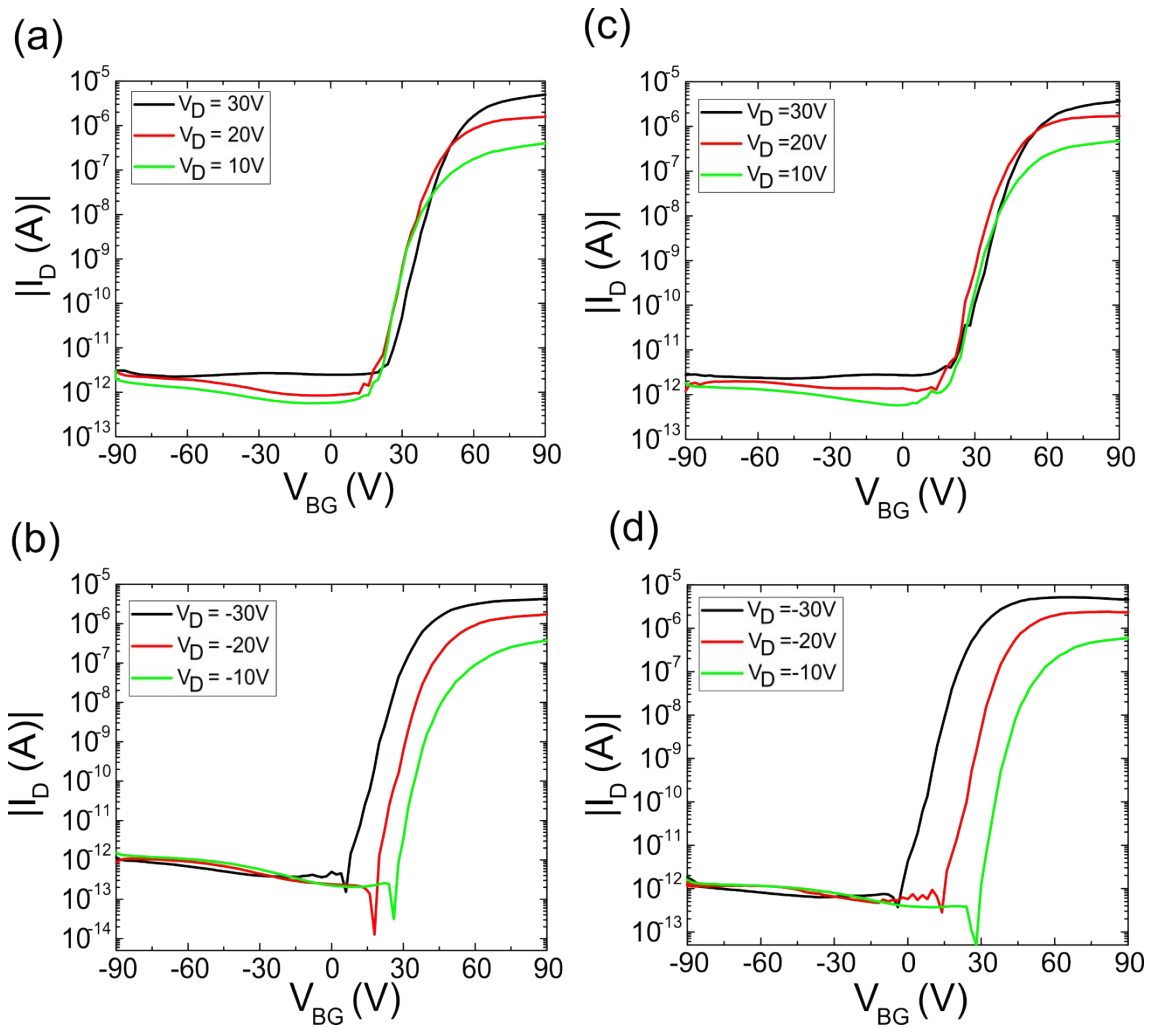


Figure S3. Transfer characteristics of anisole solvent (solvent for PMMA) coated N2200 (115 nm) transistor ($L=10\ \mu\text{m}$, $W = 10\ \mu\text{m}$) probed with respect to bottom gate (a)-(b) as spun anisole, (c)-(d) baking at 180°C for 2 min. after spin-coating of anisole.

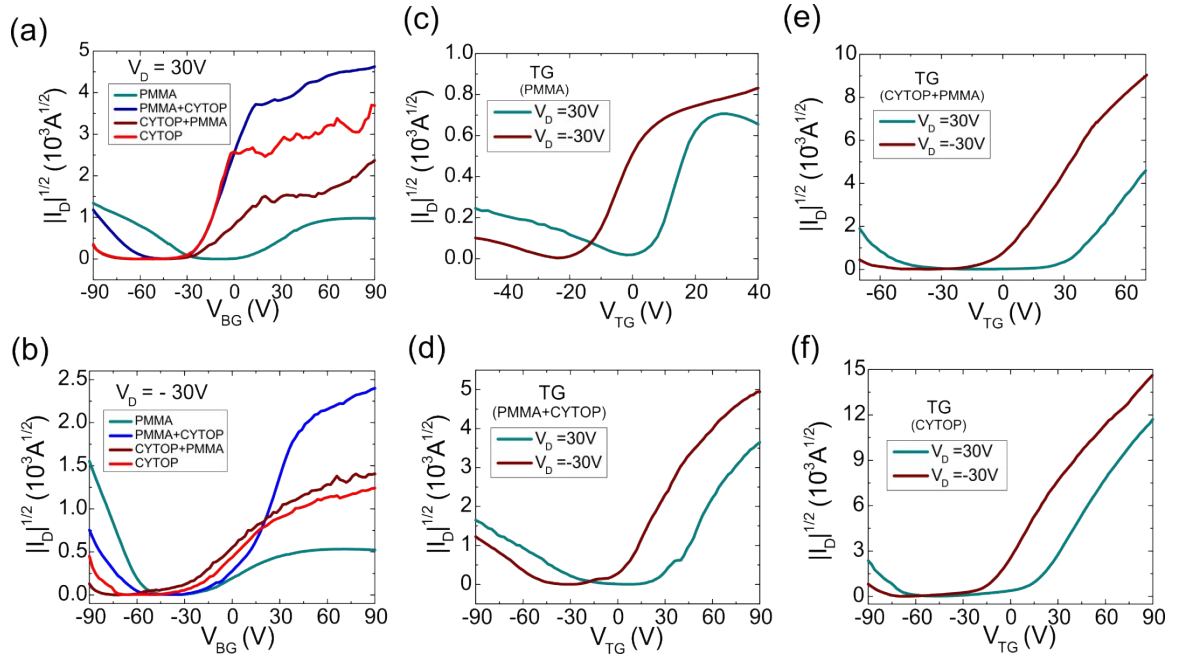


Figure S4. $\sqrt{I_D}$ vs. V_G of N2200 (36 nm) transistor ($L=10 \mu m$, $W = 10 \mu m$) probed with respect to bottom gate having different top gate dielectrics with a drain bias $V_D = 30V$ (a), with $V_D = -30V$ (b). The same with respect to top gate with different top dielectrics, (c) PMMA, (d) PMMA+CYTOP, (e) CYTOP+PMMA and (f) CYTOP.

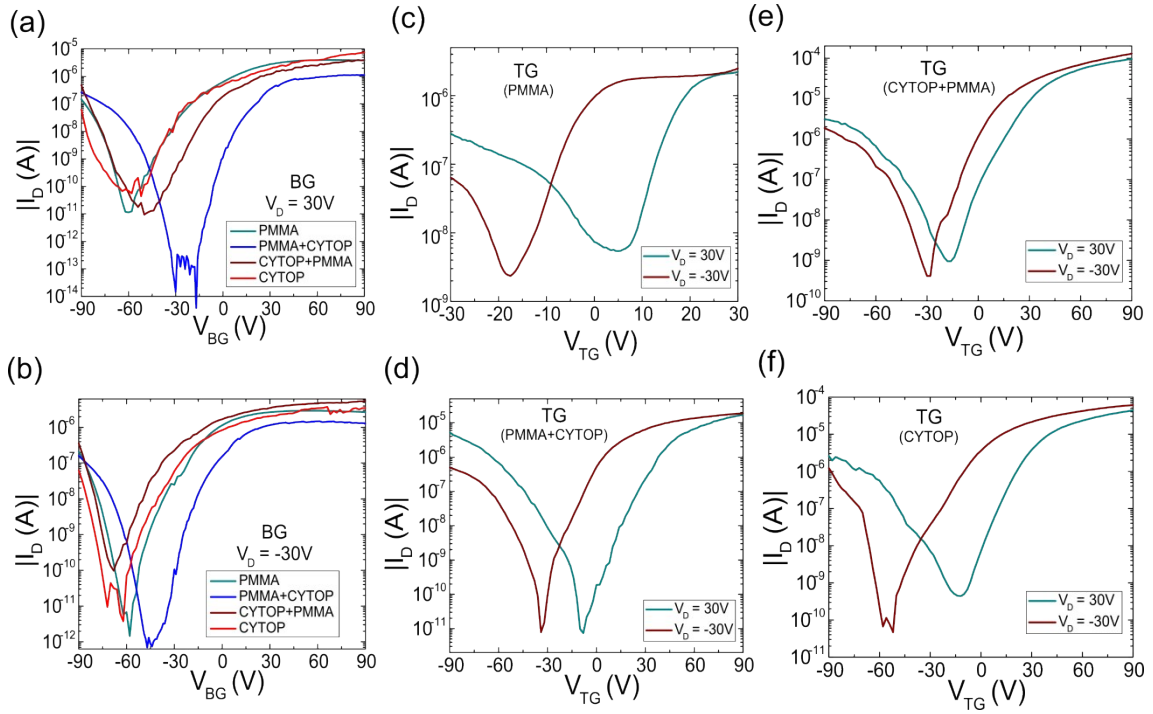


Figure S5. Transfer characteristics of N2200 (55 nm) transistor ($L=10\ \mu\text{m}$, $W = 10\ \text{nm}$) probed with respect to bottom gate having different top gate dielectrics with a drain bias $V_D = 30\text{V}$ (a), with $V_D = -30\text{V}$ (b). Transfer characteristics of the same transistors measured with respect to top gate with different top dielectrics, (c) PMMA, (d) PMMA+CYTOP, (e) CYTOP+PMMA and (f) CYTOP.

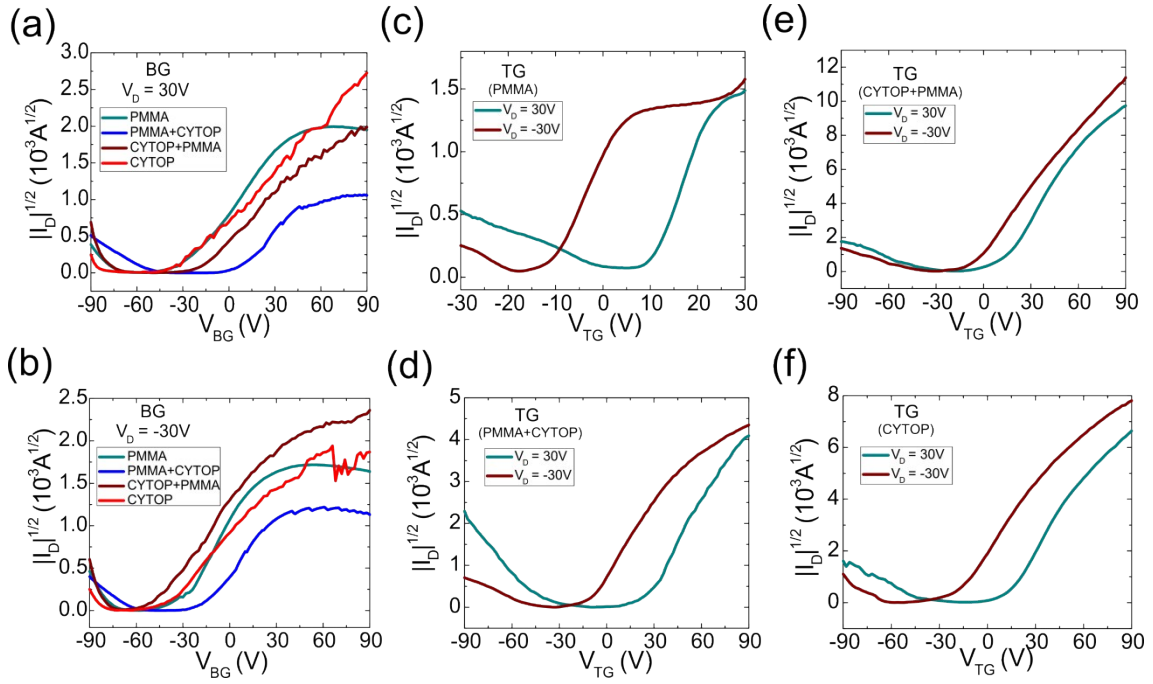


Figure S6. $\sqrt{I_D}$ vs. V_G of N2200 (55 nm) transistor ($L=10 \mu\text{m}$, $W = 10 \text{mm}$) probed with respect to bottom gate having different top gate dielectrics with a drain bias $V_D = 30\text{V}$ (a), with $V_D = -30\text{V}$ (b). The same with respect to top gate with different top dielectrics, (c) PMMA, (d) PMMA+CYTOP, (e) CYTOP+PMMA and (f) CYTOP.

Table S1a. Mobilities and turn on voltages while OFET operating in BGBC mode (with 55 nm N2200) (L=10 μm , W = 10 mm)

Top dielectrics	p-channel		n-channel	
	$\mu_{h,BG}$ ($\times 10^{-3} \text{ cm}^2 \text{ V}^{-1} \text{ s}^{-1}$)	V_{on} (V)	$\mu_{e,BG}$ ($\times 10^{-3} \text{ cm}^2 \text{ V}^{-1} \text{ s}^{-1}$)	V_{on} (V)
PMMA	0.11	-61.5	0.17	-59.6
PMMA+CYTOP	0.02	-49.2	0.18	-18.2
CYTOP+PMMA	0.41	-68.8	0.10	-48.4
CYTOP	0.08	-72.1	0.11	-52.4

Table S1b. Mobilities and turn on voltages while OFET operating in TGBC mode (with 55 nm N2200) (L=10 μm , W = 10 mm)

Top dielectrics	p-channel		n-channel	
	$\mu_{h,TG}$ ($\times 10^{-3} \text{ cm}^2 \text{ V}^{-1} \text{ s}^{-1}$)	V_{on} (V)	$\mu_{e,TG}$ ($\times 10^{-3} \text{ cm}^2 \text{ V}^{-1} \text{ s}^{-1}$)	V_{on} (V)
PMMA	0.05	-18.4	1.8	5.6
PMMA+CYTOP	0.39	-34.3	5.36	-8.2
CYTOP+PMMA	0.65	-29.5	14.40	-16.5
CYTOP	1.40	-58.1	5.52	-11.4

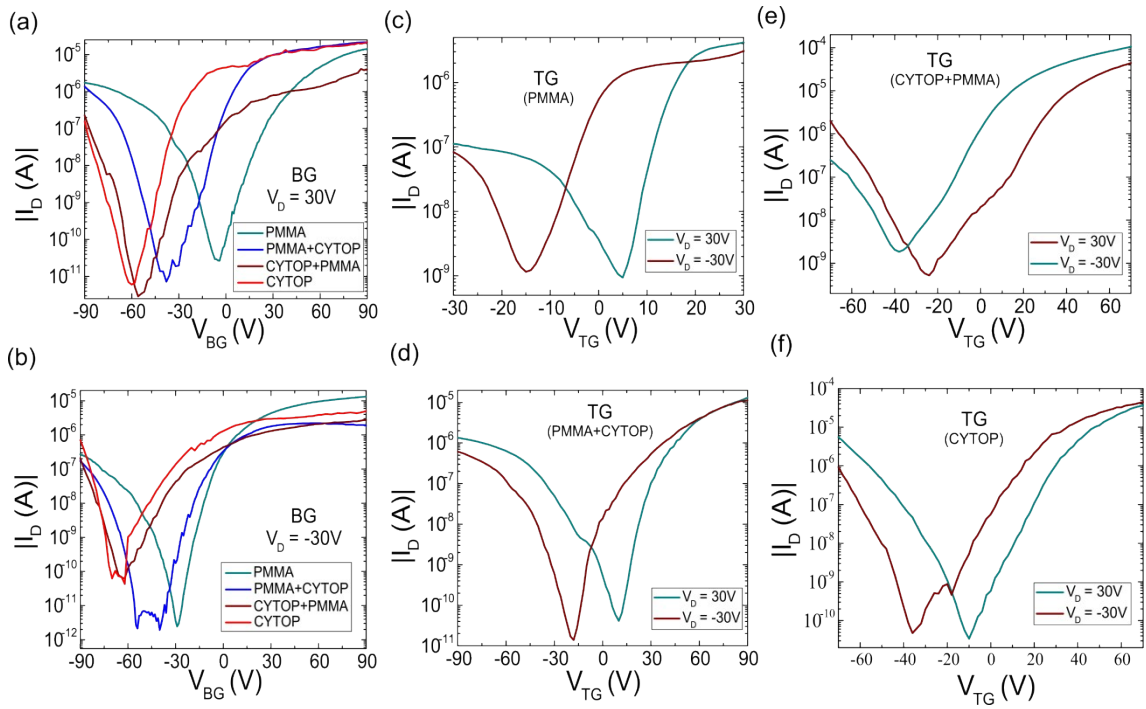


Figure S7. Transfer characteristics of N2200 (115 nm) transistor ($L=10\ \mu\text{m}$, $W = 10\ \text{nm}$) probed with respect to bottom gate having different top gate dielectrics with a drain bias $V_D = 30\text{V}$ (a), with $V_D = -30\text{V}$ (b). Transfer characteristics of the same transistors measured with respect to top gate with different top dielectrics, (c) PMMA, (d) PMMA+CYTOP, (e) CYTOP+PMMA and (f) CYTOP.

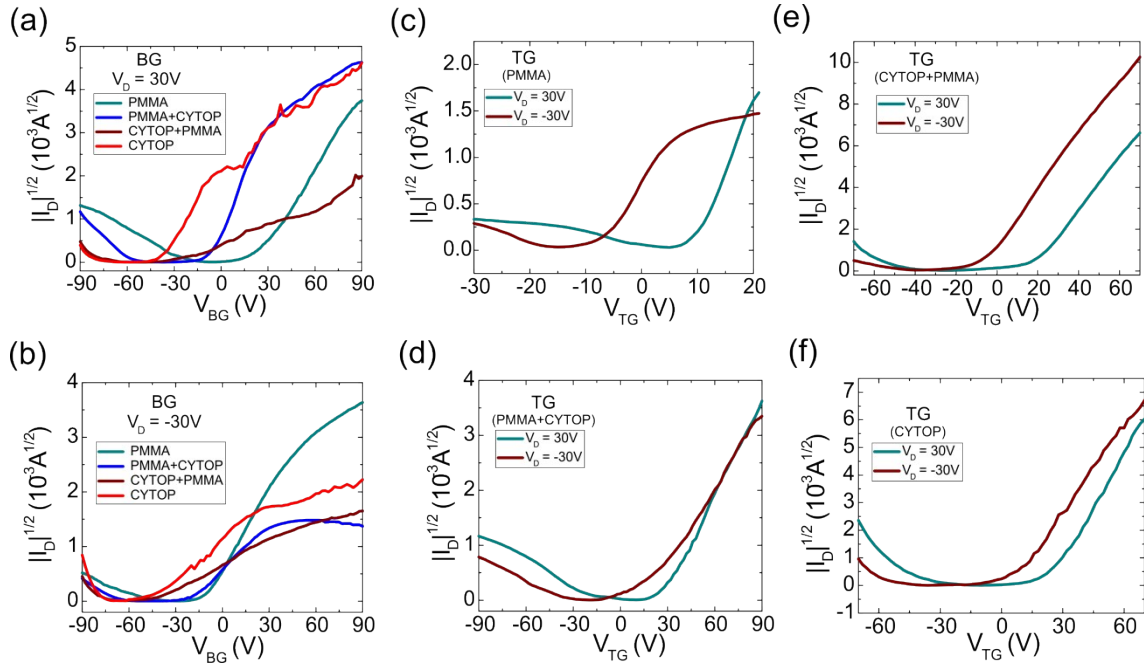


Figure S8. $\sqrt{I_D}$ vs. V_G of N2200 (115 nm) transistor ($L=10 \mu m$, $W = 10 \mu m$) probed with respect to bottom gate having different top gate dielectrics with a drain bias $V_D = 30V$ (a), with $V_D = -30V$ (b). The same with respect to top gate with different top dielectrics, (c) PMMA, (d) PMMA+CYTOP, (e) CYTOP+PMMA and (f) CYTOP.

Table S2a. Mobilities and turn on voltages while OFET operating in BGBC mode (with 115 nm N2200) (L=10 μm , W = 10 mm)

Top dielectrics	p-channel		n-channel	
	$\mu_{h,BG}$ ($\times 10^{-3} \text{ cm}^2 \text{ V}^{-1} \text{ s}^{-1}$)	V_{on} (V)	$\mu_{e,BG}$ ($\times 10^{-3} \text{ cm}^2 \text{ V}^{-1} \text{ s}^{-1}$)	V_{on} (V)
PMMA	0.03	-28.7	0.59	-4.8
PMMA+CYTOP	0.03	-53.8	1.15	-38.2
CYTOP+PMMA	0.17	-64.3	0.04	-55.1
CYTOP	0.79	-70.2	0.58	-59.6

Table S2b. Mobilities and turn on voltages while OFET operating in TGBC mode (with 115 nm N2200) (L=10 μm , W = 10 mm)

Top dielectrics	p-channel		n-channel	
	$\mu_{h,TG}$ ($\times 10^{-3} \text{ cm}^2 \text{ V}^{-1} \text{ s}^{-1}$)	V_{on} (V)	$\mu_{e,TG}$ ($\times 10^{-3} \text{ cm}^2 \text{ V}^{-1} \text{ s}^{-1}$)	V_{on} (V)
PMMA	0.02	-15.5	3.13	4.8
PMMA+CYTOP	0.10	-18.5	2.44	10.2
CYTOP+PMMA	0.21	-38.3	10.75	-24.2
CYTOP	1.87	-36.4	8.11	-10.2

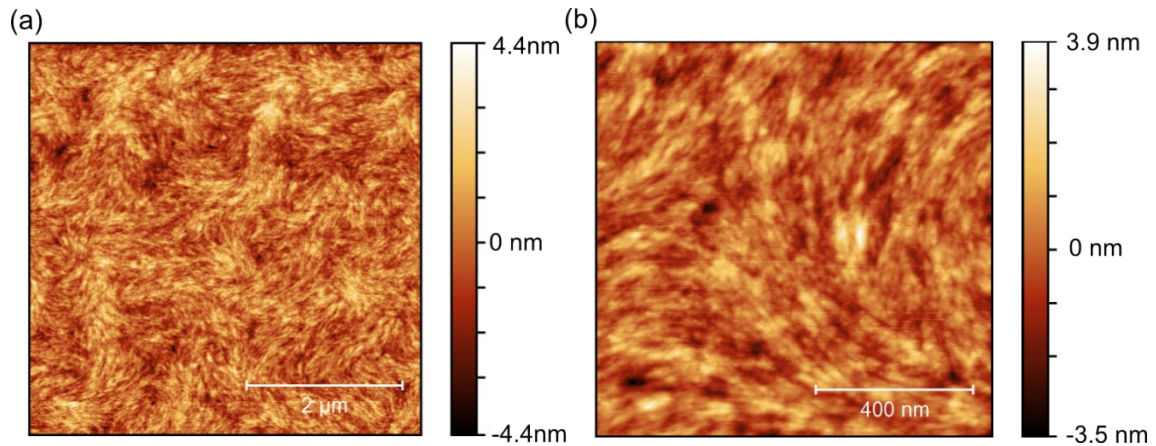


Figure S9. AFM images of N2200 film on $\text{Si}^{n++}/\text{SiO}_2$. The nodular like morphology is observed which is the characteristic growth process of this type of polymer by spin-coating. The RMS roughnesses are 0.9 nm and 0.8 nm for (a) and (b) respectively.

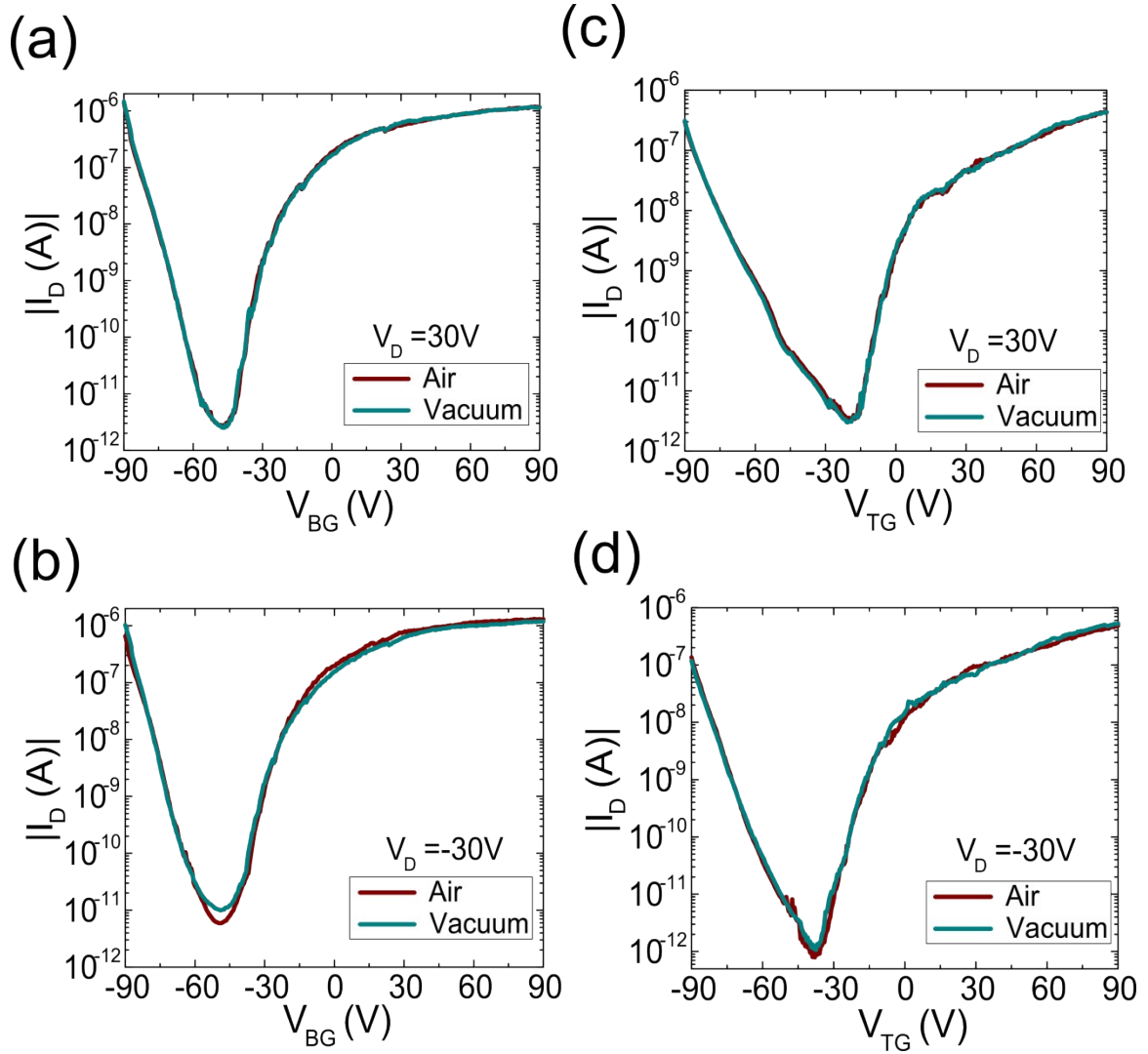


Figure S10. Air stability of dual gated N2200 transistor. Transfer characteristics of a N2200 (115 nm) transistor ($L=10\ \mu\text{m}$, $W = 10\ \text{mm}$) with PMMA+CYTOP as top gate dielectric measured in air and vacuum after 312 days of sample fabrication (sample was stored in a nitrogen filled box). Sample probed with respect to bottom gate (a) for $V_D = 30\text{V}$, (b) for $V_D = -30\text{V}$, probed with respect to top gate (c) for $V_D = 30\text{V}$, (d) for $V_D = -30\text{V}$.